AIIM

Association for Information and Image Management

1100 Wayne Avenue, Suite 1100
Silver Spring, Maryland 20910

301/587-8202

Centimeter

1 2 3 4 5 6 7 8 9 10 11 12 13 14 15 mm

1 2 3 4 5

Inches

1.0 1.1 1.25 1.4 1.6 1.8 2.0 2.2 2.5 2.8 3.2 3.6 4.0 4.5 5.0 5.6

MANUFACTURED TO AIIM STANDARDS
BY APPLIED IMAGE, INC.

1 of 1

WHC-SA-2261-FP

Irradiation Performance of Fast Flux Test Facility Drivers Using D9 Alloy

A. L. Pitner
B. C. Gneiting
F. E. Bard

Date Published
June 1994

To Be Presented at
1994 ANS Annual Meeting
New Orleans, Louisiana
June 19-23, 1994

Prepared for the U.S. Department of Energy
Assistant Secretary for Nuclear Energy

Westinghouse Hanford Company
P.O. Box 1970
Richland, Washington 99352

Hanford Operations and Engineering Contractor for the
U.S. Department of Energy under Contract DE-AC06-87RL10930

Approved for Public Release

MASTER

DISTRIBUTION OF THIS DOCUMENT IS UNLIMITED

IRRADIATION PERFORMANCE OF FFTF DRIVERS USING D9 ALLOY

A. L. Pitner, B. C. Gneiting, and F. E. Bard

Westinghouse Hanford Company
P.O. Box 1970
Richland, Washington 99352

ABSTRACT

Six test assemblies similar in design to the FFTF driver assembly but employing the advanced alloy D9 in place of Type 316 stainless steel for duct, cladding, and wire wrap material were irradiated to demonstrate the improved performance and lifetime capability of this design. A single pinhole-type breach was incurred in one of the high exposure tests after a peak fuel burnup of 155 MWd/kgM and peak fast neutron fluence of 25 x 10^{22} n/cm^2 (E > 0.1 MeV). Postirradiation examinations were performed on four of the test assemblies and measured results were compared to analytical evaluations. A revised swelling correlation for D9 Alloy was developed to provide improved agreement between calculated and measured cladding deformation results. A fuel pin lifetime design criterion of 5% calculated hoop strain was derived. Alternatively, fuel pin lifetimes were developed for two irradiation parameters using statistical failure analyses. For a 99.99% reliability, the analyses indicated a peak fast fluence lifetime of 21.0 x 10^{22} n/cm^2, or a peak fuel burnup greater than 120 MWd/kgM. The extended lifetime capability of this design would reduce fuel supply requirements for the FFTF by a third relative to the reference driver design.

1.0 INTRODUCTION

The reference driver fuel assembly (DFA) in the Fast Flux Test Facility (FFTF) utilizes mixed oxide (MOX) fuel pellets and Type 316 stainless steel (SS) for duct, cladding, and wire wrap material. The 217 fuel pins, each 0.230 in. (5.84 mm) diameter, are contained in a hexagonal duct tube, which is attached to a shield/orifice assembly at the bottom and a handling socket at the top, as shown in Figure 1. While operating experience has demonstrated that this fuel design easily meets its 80 MWd/kgM design burnup goal,[1] it is apparent that the ultimate lifetime capability of these fuel assemblies is limited by cladding and duct distortion caused by irradiation-induced swelling and creep. Swelling in Type 316 SS becomes prevalent once the incubation period for the onset of swelling is exceeded. The advanced alloy D9 shows improved swelling behavior compared to 316 SS in that the onset of swelling is delayed to higher exposure levels. Six D9 test assemblies have accordingly been irradiated in the FFTF to demonstrate the extended lifetime capability of this potential DFA design. The fuel pin and assembly designs for these six tests were similar to the reference DFA design for the FFTF,[2] except that D9 alloy was substituted for Type 316 SS for duct, cladding, and wire wrap components. Detailed postirradiation examinations were performed on four of the test assemblies.

2.0 IRRADIATION TESTING

The initial loading pattern for the six D9 test assemblies in the FFTF core is shown in Figure 2. Some of the assemblies were relocated during later irradiation cycles to maintain target test conditions.

The calculated peak operating conditions and exposure levels for the test assemblies are presented in Table 1. Fast fluence values refer to neutrons with $E > 0.1$ MeV. As indicated in Table 1, only one cladding breach was incurred in this irradiation test series. A cladding breach in the D9-2 test was detected by fission gas monitors after 775 equivalent full power days (EFPD) of irradiation, with a peak assembly burnup of 155 MWd/kgM and a peak assembly fast fluence of 25×10^{22} n/cm^2 ($E > 0.1$ MeV). There was no delayed neutron signal associated with the breach event, indicating that fuel was not

in direct contact with the reactor coolant. Postirradiation examination revealed the failure to be a pinhole type breach at an axial location of 56% of the fuel column height (X/L = 0.56, where X/L=0 is the bottom and X/L=1 is top of the fuel column). The breach was at the location of peak cladding strain in the pin. The pin that failed was calculated to be the hottest in the pin bundle. There were no pin failures in any of the other tests, including the D9-3 test which was irradiated to a higher exposure level than the D9-2 test, albeit at lower fuel pin power levels.

Figure 3 presents the coolant outlet temperature histories (top of the fuel column) for typical high temperature pins in each of the test assemblies that were examined. These temperatures were determined from measured assembly bulk coolant outlet temperatures and calculated temperature distributions within the pin bundles. The bundle average outlet temperatures were about 40 °F (22 °C) less than the values indicated in the figure.

3.0 POSTIRRADIATION MEASUREMENTS

3.1 Assembly Ducts

The FFTF has the capability of measuring individual assembly elevations during reactor shutdown periods using an In-Vessel Handling Machine (IVHM) located in each tri-sector of the reactor core. These measurements reflect axial duct growth caused by irradiation-induced volume swelling in these components. The reported accuracy of these measurements is $\pm$0.028 in. (0.71 mm),[3] and the measurements have been substantiated by ex-reactor examinations performed on discharged assemblies. Figure 4 presents the results of such measurements taken on both 316 SS- and D9-ducted assemblies irradiated in the FFTF, where the axial growths are plotted against calculated peak fast fluence levels. Scatter in the data is at least partially due to operating temperature differences and the associated dependence of irradiation-induced swelling behavior on temperature. Despite the data scatter, the improved performance in duct growth behavior for D9 assemblies is quite evident. For Type 316 SS, duct growth becomes prevalent once the fast neutron fluence exceeds about 5×10^{22} n/cm^2. Growth of the D9 assemblies is delayed because of the longer incubation period for the onset of void swelling

in this material, and does not become prevalent until the fast fluence exceeds about 10 x 10^{22} n/cm^2.

3.1 Fuel Pins

The measured strain profile for the fuel pin that breached in the D9-2 test is shown in Figure 5, where diametral cladding strain is plotted against axial position. The general profile shape shown here is representative of most of the fuel pins examined in this test series. Some degree of fuel cladding mechanical interaction (FCMI) is evident near the bottom of the fuel column. The perturbations in the strain profile near the top of the fuel column are attributed to interaction with fission products that relocate to this region. Peak cladding strain occurred near the fuel column midplane. The breach occurred essentially at the peak strain location, where the measured strain level was 12.7%. A number of other pins in the D9-2 test bundle incurred larger strains without cladding breach. The largest measured cladding strain in the D9-2 test was 13.5%.

Total cladding diametral strain is a product of irradiation induced swelling and in-reactor creep. To determine the swelling component of the measured total strain, immersion density measurements were made on cladding segments at various axial locations (irradiation creep causes insignificant density change). The results shown in Figure 6 confirm that the majority of cladding deformation in the high strain region is due to void swelling as expected.

The collective set of peak cladding strains measured in the four tests examined are plotted against peak fast fluence values in Figure 7. The trend of increasing strain with increasing irradiation exposure is clearly evident. Strain levels in excess of 13% were incurred near an exposure level of 25 x 10^{22} n/cm^2. The D9-3 test reached a peak fast fluence of 27 x 10^{22} n/cm^2 without a cladding breach, but was not examined due to program redirection.

A corresponding presentation of measured pin axial growths as a function of peak fast fluence is shown in Figure 8. The trend previously measured for 316 SS fuel pins[4] is included for comparison. The largest D9 growth values

shown represent over 5% of the fuel column height. There was a definite correspondence between peak cladding strain and pin axial growth for all pins examined, as shown in Figure 9. Such correlation is not unexpected since the dominant factor affecting pin deformation is generally fluence. Axial pin growth reflects an integrated irradiation-induced swelling value, which is mainly fluence dependent. The diametral strains include a swelling contribution (which is dominant) and a creep strain contribution, which again is dominated by fluence-dependent irradiation creep.

Fuel column growths were determined from neutron radiographs of the pins examined after reactor irradiation. Frequently, gaps between pellets in the fuel columns were discernible in the radiographs. In Figure 10, the measured fuel column growth is plotted against the corresponding pin axial growth for all pins examined in this test series. A definite correlation between these parameters is apparent in the data, especially for the higher burnup tests. It appears that the fuel column essentially follows the cladding as it extends axially due to irradiation-induced swelling.

A number of fuel pins were punctured to measure fission gas release quantities. In Figure 11, the measured fractional gas release values are presented as a function of peak fuel burnup. The gas release correlation in the SIEX4 code, which is used for analytical evaluations of fast reactor fuel pins, is also shown in the figure. SIEX4 is an updated version of the SIEX3 code,[5] and has the same gas release correlation. The results confirm that gas release is nearly complete at the higher burnup levels, as projected by the SIEX4 correlation.

4.0 ANALYTICAL EVALUATIONS

4.1 Cladding Deformation

All the fuel pins that were examined after irradiation were analyzed using the both the SIEX4[5] and LIFE-4[6] computer codes, and calculated cladding strain behavior was compared to measured strain profiles. In general, the code calculations agreed well with one another, and it was decided that only the more simplistic SIEX4 analyses need be performed in

future evaluations. Calculated strain behavior was in reasonable agreement with measured results using the current swelling and creep correlations, but some deficiencies were noted. Cladding strain levels were typically undercalculated in the lower fuel column region, and there sometimes were significant differences between calculated and measured peak cladding strain levels. In particular, the peak cladding strains in the high exposure D9-2 test were undercalculated by about 2%, which represents a non-conservative analytical assessment. Since a major goal of analytical evaluations is to conservatively estimate fuel pin lifetime limits, it was deemed prudent to improve the agreement between calculated and measured results for this high exposure data set.

Only minor modifications were made to the current swelling correlation for D9 alloy to achieve improved agreement with measured cladding strain profiles. The same analytical formulation was maintained, with small adjustments made to the temperature-dependent expression and swelling rate magnitude. The peak swelling temperature was reduced from 783 K to 773 K, and the fluence dependent swelling rate term was increased by 8%. The improved agreement attained between calculated and measured strain profiles is typified in Figure 12, which compares the calculations using the old and new swelling correlation to the measured profile for the failed pin in the D9-2 test. With the new correlation, the general shape of the strain profile is better matched and the peak cladding strain near the core midplane in the area of the cladding breach is better calculated.

The peak cladding strains calculated with the revised swelling correlation are compared in Figure 13 against measured values for all the pins examined. Also shown in the figure are two straight line fits obtained by regression analyses of results produced by both the old and new swelling correlations. The fitted line for the new correlation is seen to lie closer to the ideal "Calculated = Measured" line, indicated by the dashed line in the figure. The agreement between calculated and measured strains for the high exposure D9-2 test is reasonably good with the new correlation, which was one of the objectives for revision of the swelling correlation. Statistically, the average difference (and standard deviation of the differences) between calculated and measured peak cladding strains for the entire 89-pin data set

was improved from -0.85% $\Delta D/D$ ($\pm$1.23% $\Delta D/D$) for the old correlation to +0.04% $\Delta D/D$ ($\pm$1.12% $\Delta D/D$) for the new correlation.

4.2 Weibull Analysis

Fuel pin lifetime estimates can be made for different fuel designs irradiated in the FFTF using Weibull failure analysis techniques.[7] The procedure combines failure and non-failure data points to project reliability as a function of an appropriate aging parameter. The Weibull procedure provides a simple graphical solution consisting of plotting a curve and analyzing it. The horizontal axis is the aging parameter (selected as fast neutron fluence for this evaluation), and the vertical scale is the probability of failure. The slope of the line can represent a failure mode indicative of infant mortality, early life wearout, or old age rapid wearout.

The Weibull analysis can provide useful results with limited data, such as small sample populations. However, at least two failure points are required to define the Weibull curve. Since there was only a single cladding breach in this D9 test series, an artificial failure point was introduced into the data set. To select the artificial failure point, it was assumed that the failure mode for D9 fuel pins was the same as for similar 316 SS fuel pins, for which more failure data are available.[2] Specifically, an artificial failure point close to the peak fast fluence of the D9-3 test was selected to provide the same slope as for the Weibull analysis of the 316 SS pins. The results of this procedure are shown in Figure 14. At a target reliability of 99.99% (one failure in ten thousand), the Weibull analyses indicate the fast fluence lifetime is increased from 14.4×10^{22} n/cm^2 for 316 SS to 21.0×10^{22} n/cm^2 for D9.

4.3 Fuel Pin Lifetime Design Criterion

A number of different design procedures can be applied in assessing lifetime performance capabilities and limits for liquid metal reactor fuel pins. Common approaches used in the past have included inelastic creep strain limits and calculation of the cumulative damage fraction (CDF). The results

of this study indicate another design procedure could be used, one that is based on total cladding strain (swelling and creep) limits. For austenitic stainless steel type cladding, total strain at high exposures is generally dominated by irradiation-induced void swelling effects. A failure mechanism associated with this void swelling is identified as channel fracture.[8] This is a non-ductile type failure in which the material fails in "channels" associated with the distributed voids produced by irradiation swelling. Channel fracture has been observed in various types of austenitic stainless steels with volumetric void-swelling values in excess of 10% (~3.3% $\Delta D/D$).

A viable total strain criterion for lifetime evaluations of D9 fuel pins was developed from the combined results of the Weibull analyses and the known statistical accuracy of calculated cladding strains for this data set. At the 95% confidence limit for SIEX4 calculations of total cladding strain, operation in a mode of low fuel pin failure probability (1 pin in 10,000) is assured so long as the calculated peak cladding total diametral strain does not exceed 5% $\Delta D/D$. This provides more specific quantification of a previously proposed limit of <10% diametral swelling to avoid brittle fracture.[9]

5.0 FUEL SUPPLY IMPLICATIONS

The extended lifetime capability of the D9 fuel design significantly reduces fuel supply requirements relative to the reference 316 SS driver design. Assuming a core loading of 74 DFAs in the FFTF and an operating capacity factor of 82% (three 100-day cycles per year), approximately 50 DFAs of the reference 316 SS design would require replacement each year. With the extended lifetime capability of the D9 design, about 33 DFAs would need to be replaced each year. This represents a one-third reduction in fuel supply requirements for the reactor.

6.0 CONCLUSIONS

Six test assemblies containing over 1300 fuel pins similar in design to the FFTF reference fuel assembly but using advanced D9 alloy in place of 316 SS for duct, cladding, and wire wrap material were irradiated to demonstrate the improved performance and lifetime capability of this design. Peak fuel burnups ranged from 101 to 188 MWd/kgM, and peak fast fluences ranged from 12 to 27 x 10^{22} n/cm^2. Only a single benign cladding breach was incurred in this test series. With slight modifications to the current D9 swelling correlation, good agreement between calculated and measured fuel pin deformation was achieved. A fuel pin lifetime design criterion was developed wherein operation in a mode of low probability for fuel pin failure (1 in 10,000) is assured so long as the SIEX4 calculated peak cladding strain does not exceed 5% $\Delta D/D$. Using fast fluence as a lifetime parameter, the performance capability is extended from 14.4 x 10^{22} n/cm^2 for the reference 316 SS driver design to 21.0 x 10^{22} n/cm^2 for the D9 design, representing a one-third reduction in fuel supply requirements.

7.0 REFERENCES

1. R. B. Baker, J. W. Hales, L. A. Lawrence, and B. J. Makenas, "Evaluation of Fast Flux Test Facility Driver Fuel Irradiated Beyond Goal Burnup," WHC-EP-0092, October 1987.

2. R. B. Baker, F. E. Bard, and J. L. Ethridge, "Performance of Fast Flux Test Facility Driver and Prototype Driver Fuels," *Proc. LMR: A Decade of LMR Progress and Promise*, Washington, D.C., November 11-15, 1990, p. 184, American Nuclear Society (1990).

3. S. L. Hecht and R. G. Trenchard, "Fast Flux Test Facility Core Restraint System Performance," WHC-SA-0683-FP, February 1990.

4. B. J. Makenas, S. A. Chastain, and B. C. Gneiting, "Dimensional Changes in FFTF Austenitic Cladding and Ducts," *Proc. LMR: A Decade of LMR Progress and Promise*, Washington, D.C., November 11-15, 1990, p. 176, American Nuclear Society (1990).

5. R. B. Baker and D. R. Wilson, "SIEX3 - A Correlated Computer Code for Predictions of Fast Reactor Mixed-Oxide Fuel and Blanket Performance," *Proc. Int. Conf. Reliable Fuels for Liquid Metal Reactors*, Tucson, Arizona, September 7-11, 1986, p. 5-40, American Nuclear Society (1986).

6. A. Biancheria, T. S. Roth, and B. E. Sundquist, "Steady State and Transient Fuel Performance Modelling: LIFE-4 Update," *Proc. Int. Conf. Reliable Fuels for Liquid Metal Reactors*, Tucson, Arizona, September 7-11, 1986, p. 5-1, American Nuclear Society (1986).

7. N. J. McCormick, "Reliability and Risk Analysis (Methods and Nuclear Power Applications)," Academic Press, New York (1981).

8. M. L. Hamilton, F. H. Huang, W. J. S. Wang, and F. A. Garner, "Influence of Radiation on Material Properties," *13th In. Symp., Part II, STP 956*, Philadelphia, Pennsylvania, p. 245, ASTM (1987).

9. R. B. Baker, F. E. Bard. R. D. Leggett, and A. L. Pitner, "Status of Fuel, Blanket, and Absorber Testing in the Fast Flux Test Facility," *J. Nucl. Matl. 204*, p. 109 (1993).

Table 1. Calculated Peak Operating Conditions and Exposures.

Test	EFPD	Peak Pin Power, kW/ft (kw/m)	Peak Cladding Temperature, °F (°C)	Peak Burnup, MWd/kgM	Peak Fast Fluence, 10^{22} n/cm^2
● C-1	468	11.9 (39.0)	1267 (686)	108	16.5
● D9-1	413	13.4 (44.0)	1121 (605)	101	15.1
● D9-2*	775	12.4 (40.7)	1081 (583)	155	25.3
D9-3	1468	10.4 (34.1)	1090 (588)	188	27.0
● D9-4	568	12.2 (40.0)	1079 (582)	124	21.4
CRBR-5	468	11.7 (38.4)	1096 (591)	113	16.6

● Postirradiation examination performed

* Test incurred breached pin

Figure 1. FFTF Fuel Assembly.

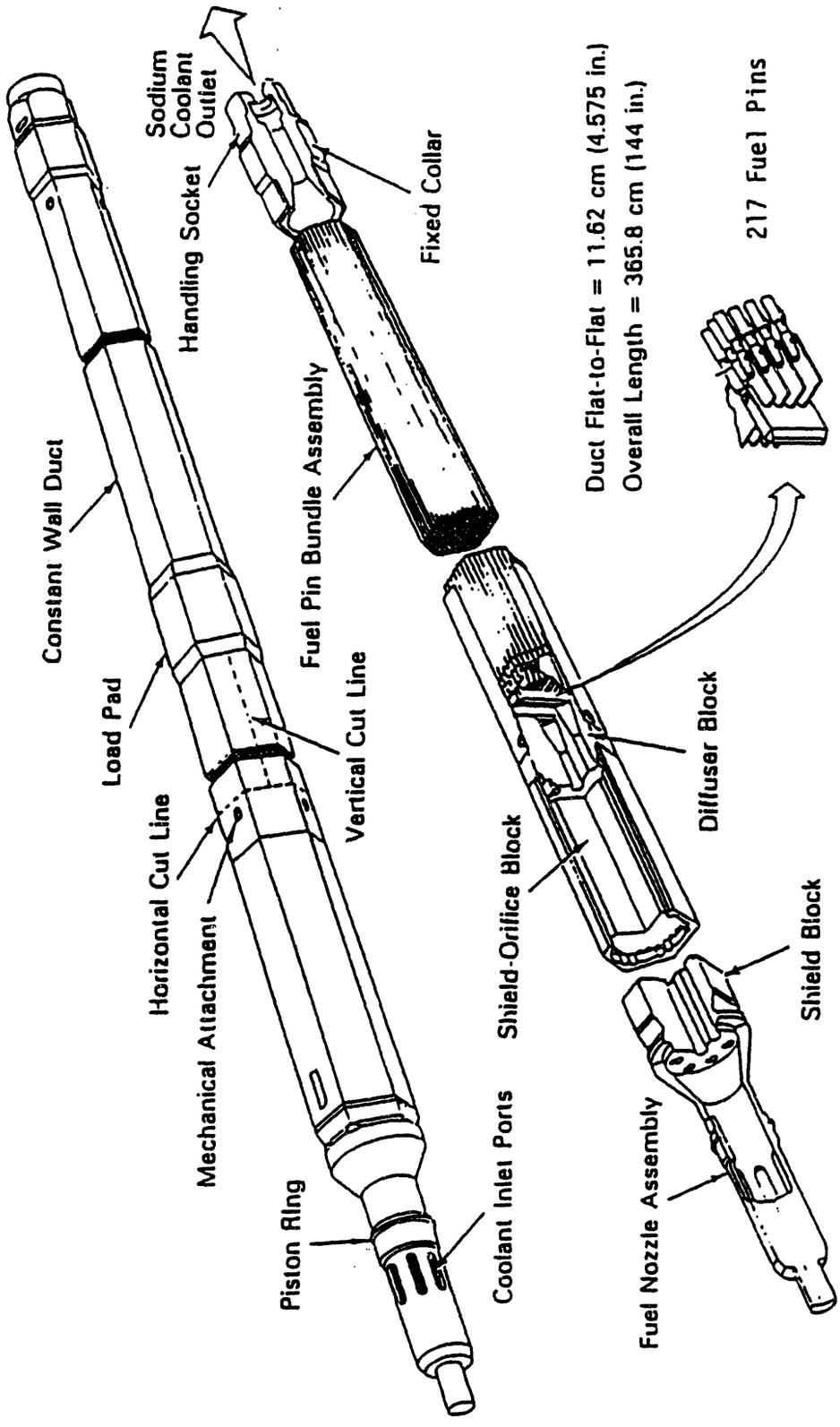

Figure 2. Test Locations in the FFTF Core.

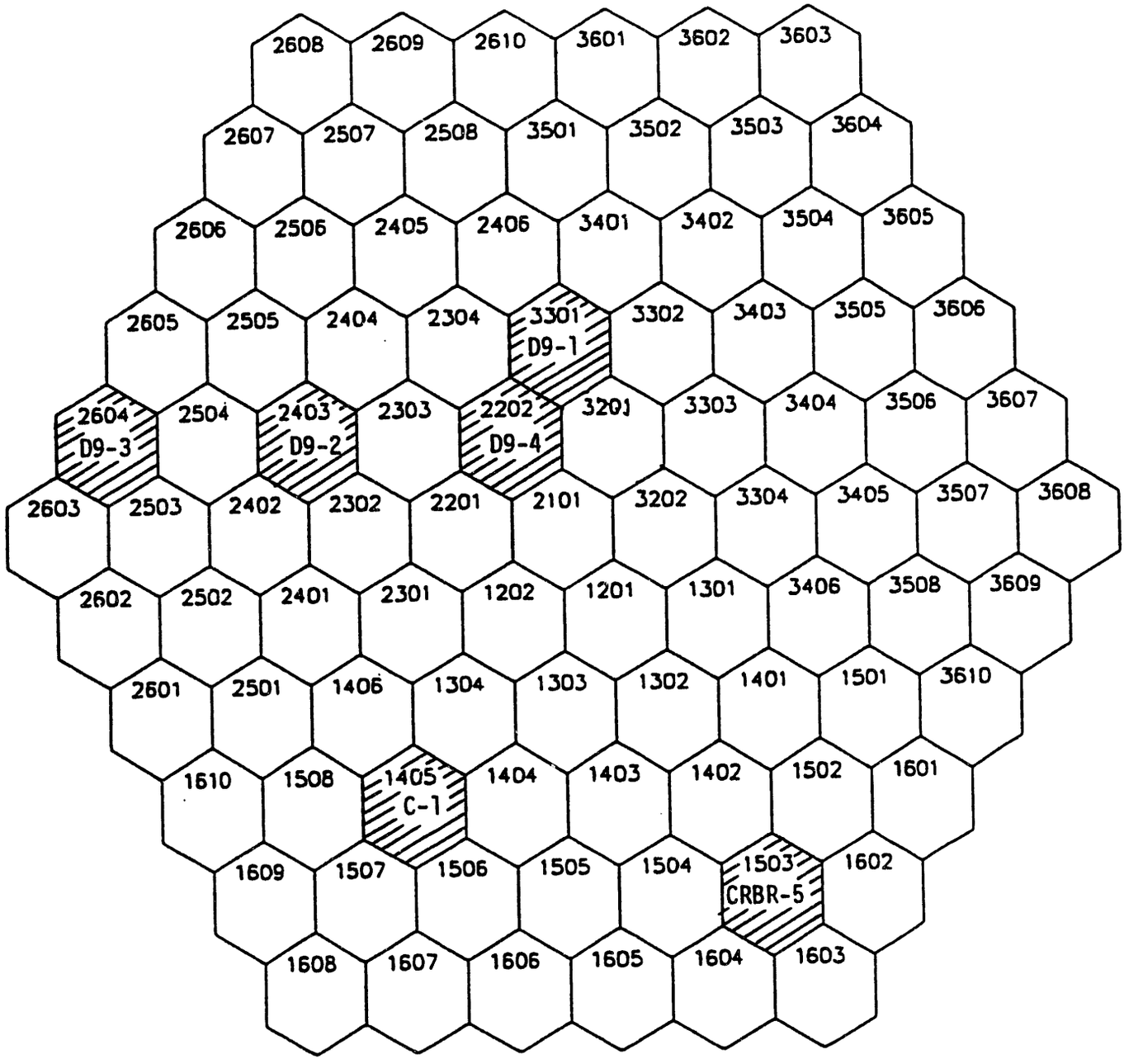

Figure 3. Coolant Outlet Temperature Histories (Top of Fuel Column).

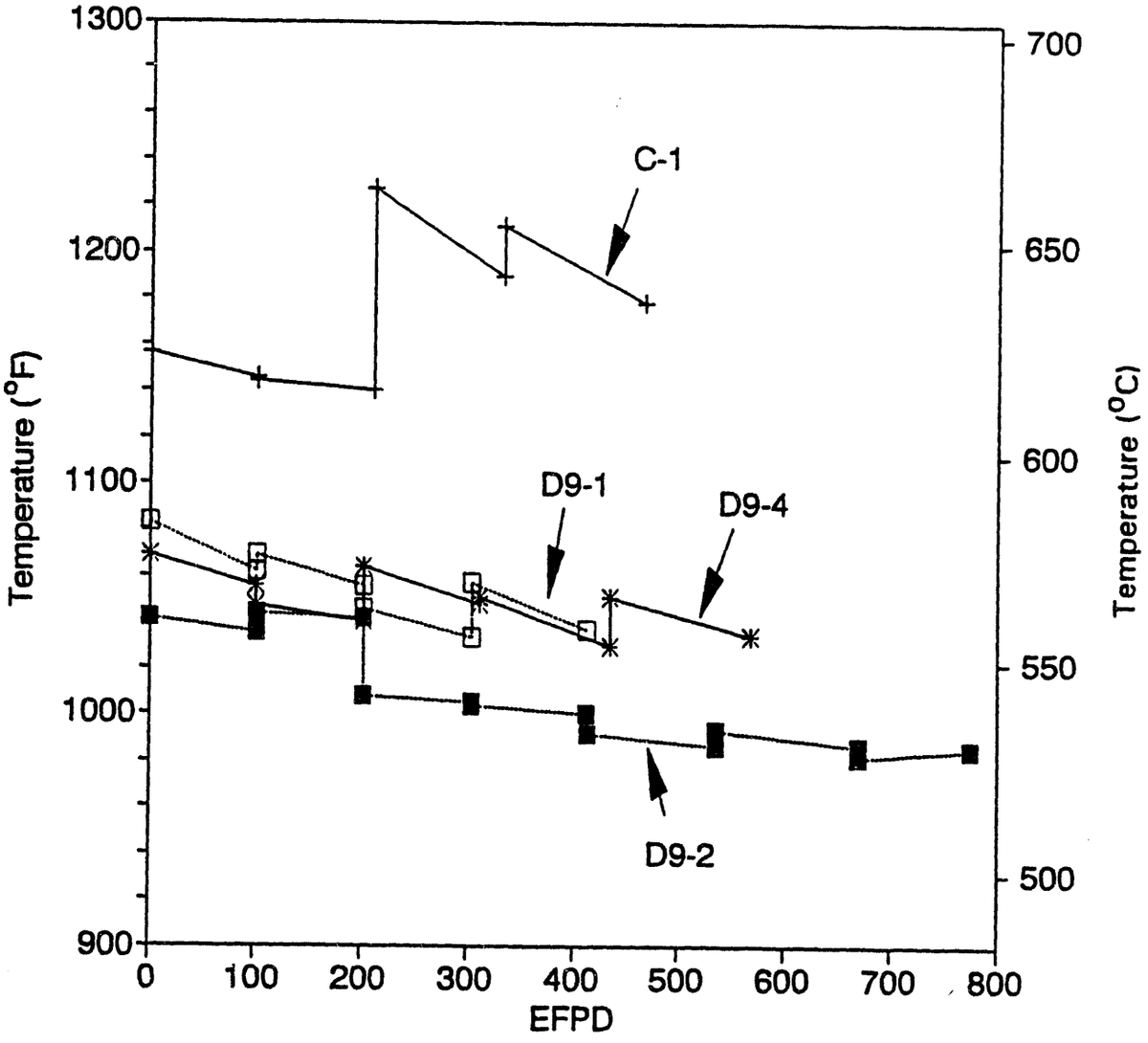

Figure 4. In-Reactor Duct Growth Measurements.

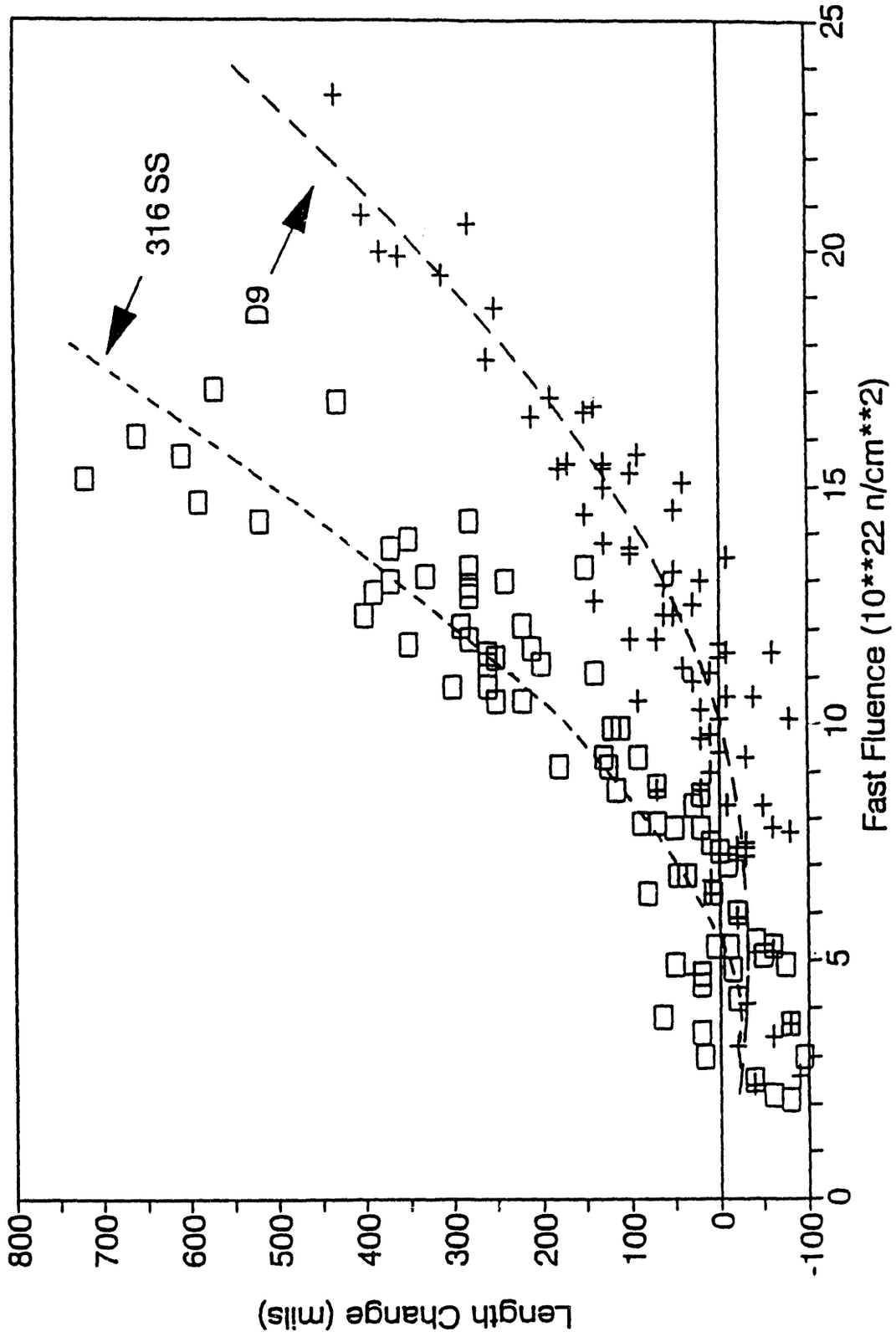

Figure 5. Measured Cladding Strain Profile for Breached Pin in D9-2 Test.

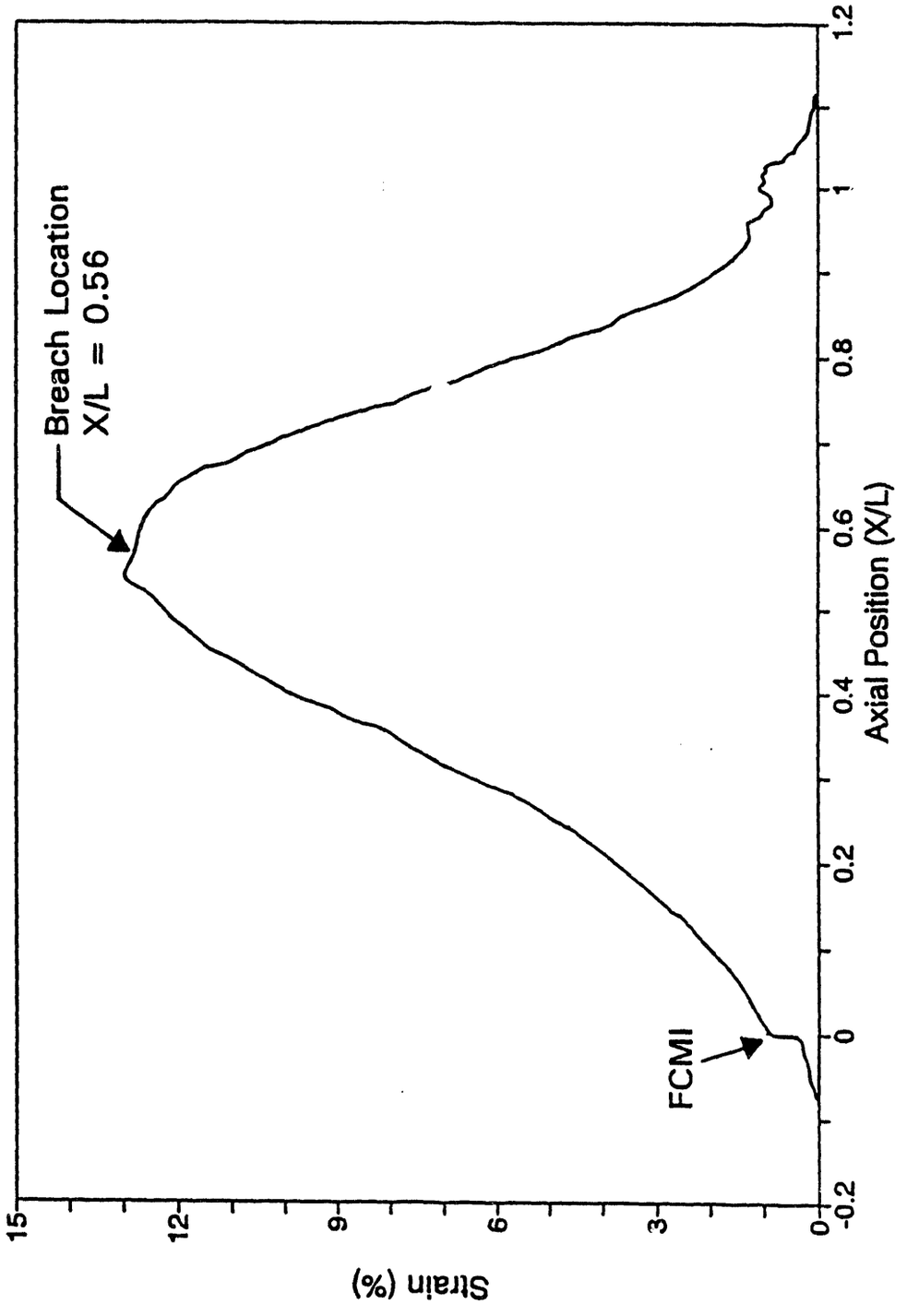

Figure 6. Measured Swelling Component of Total Cladding Strain.

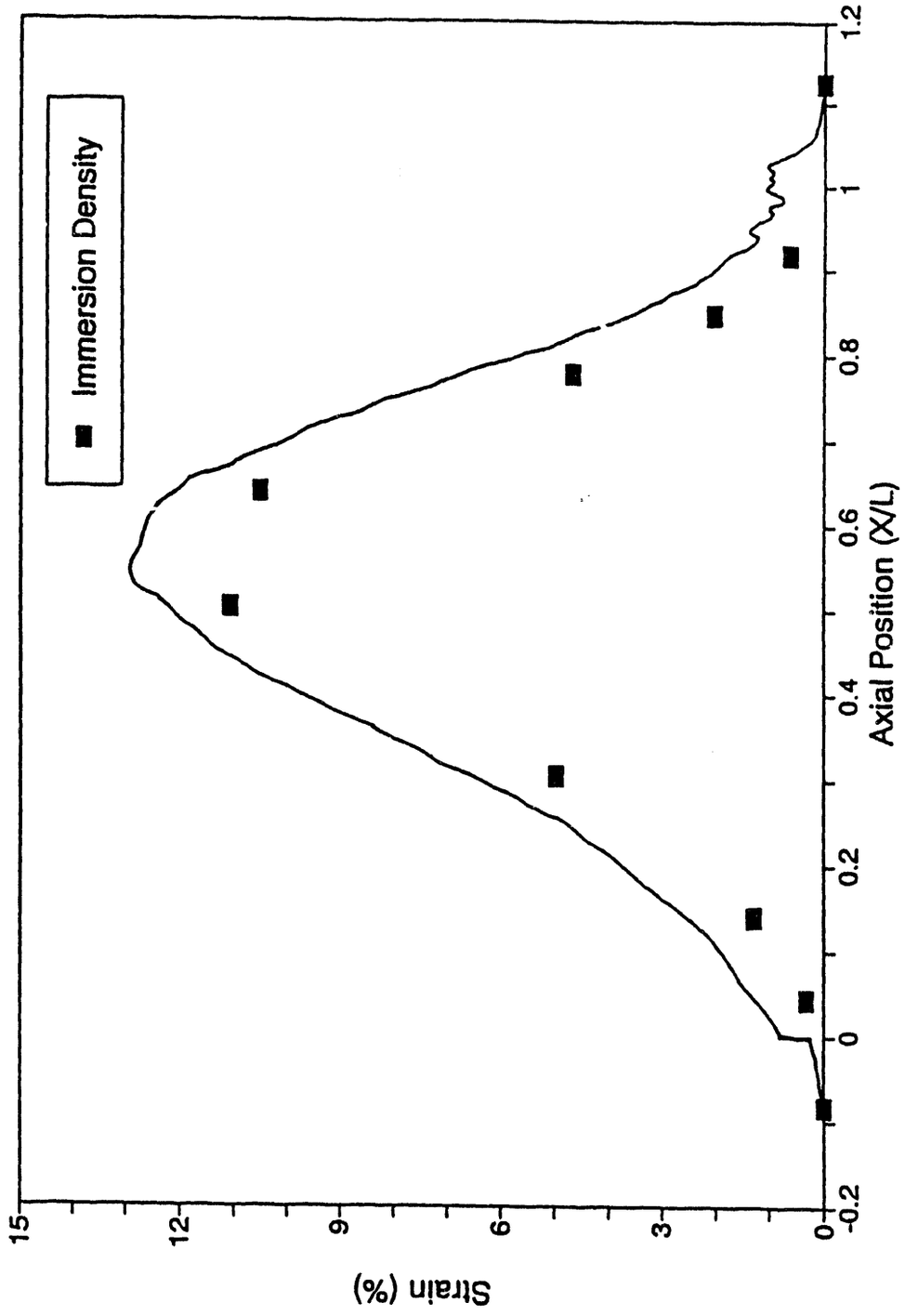

Figure 7. Measured Peak Cladding Strains Versus Fast Fluence.

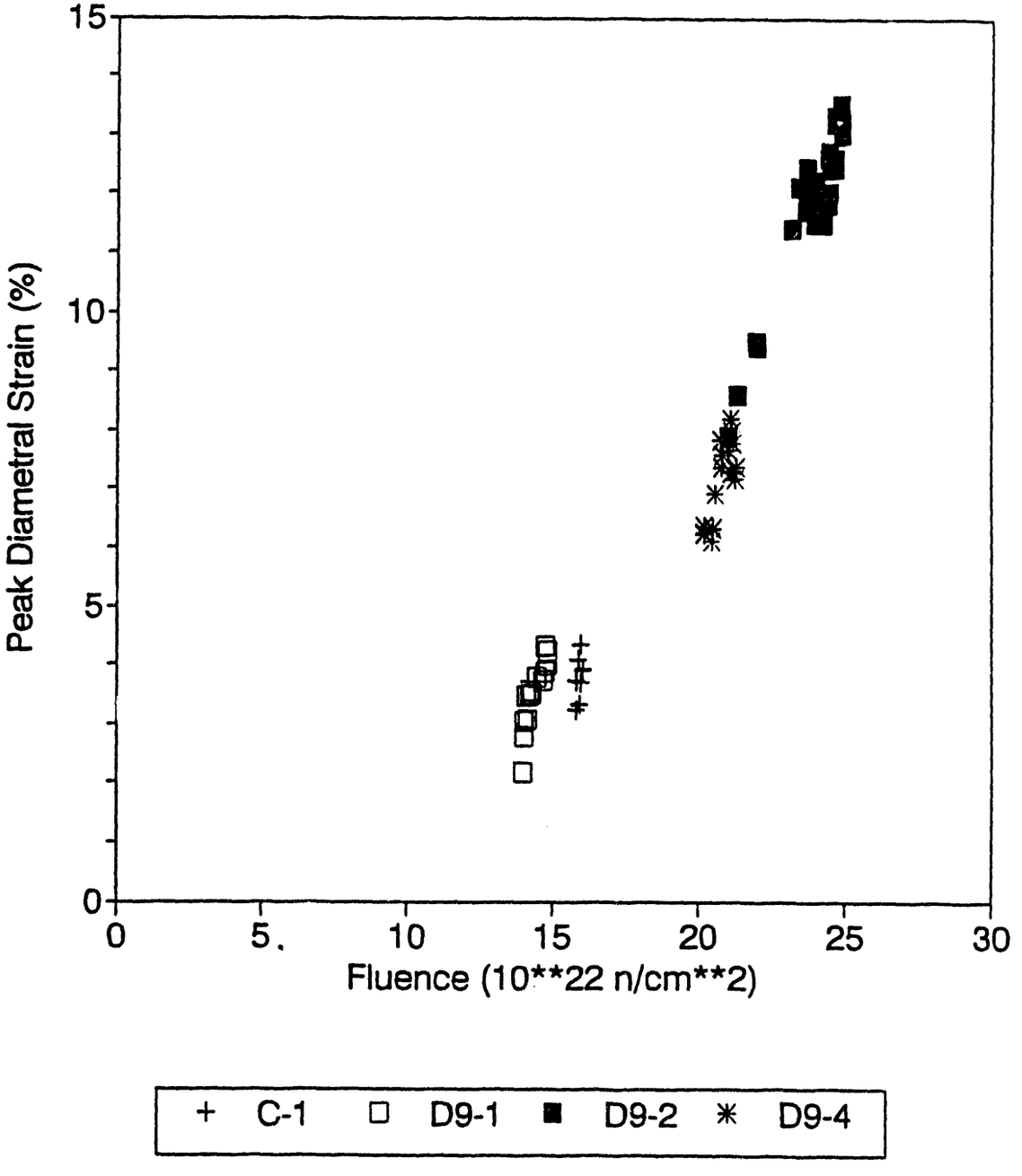

Figure 8. Measured Pin Axial Growths Versus Fast Fluence.

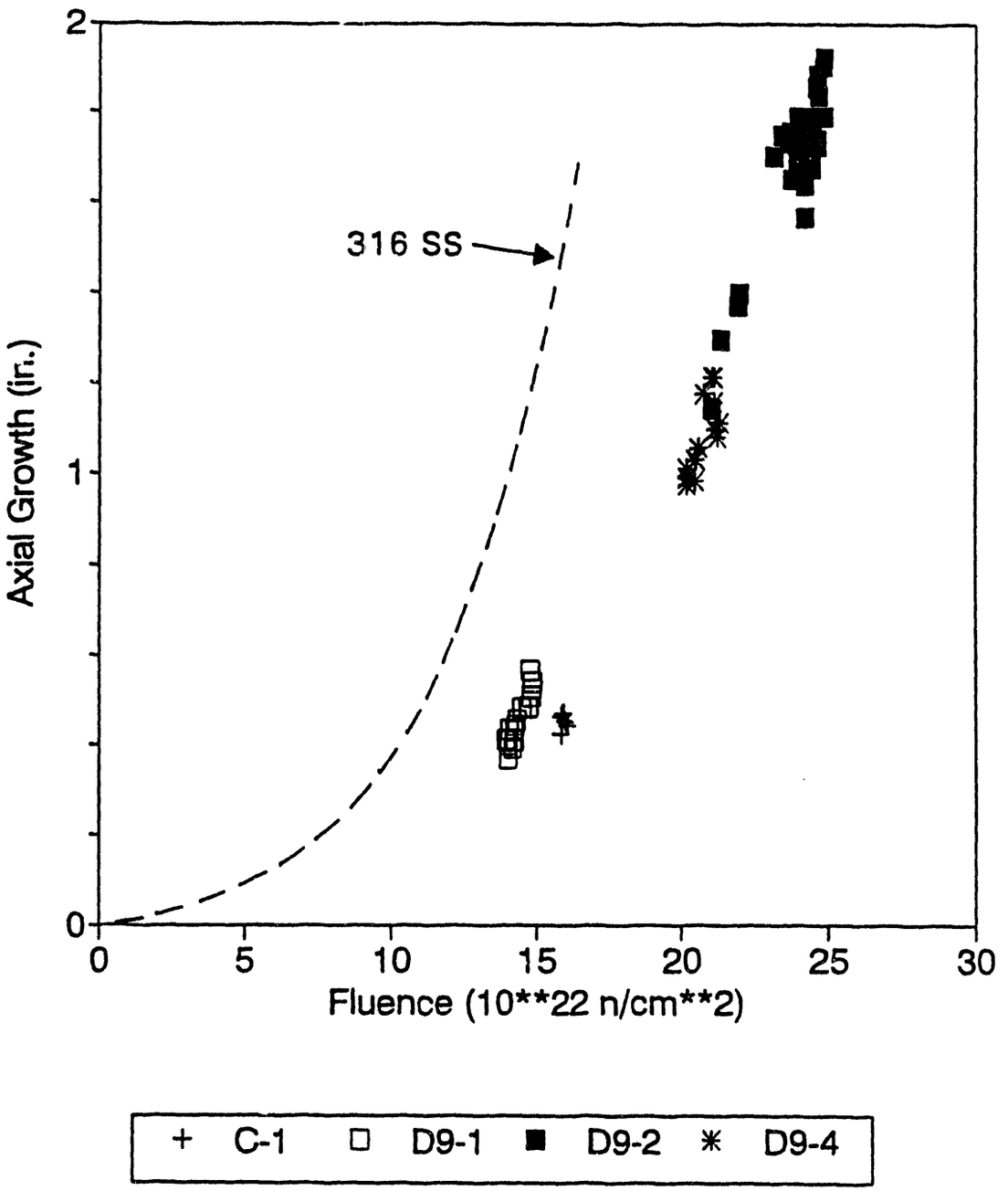

Figure 9. Peak Cladding Strain Versus Pin Axial Growth.

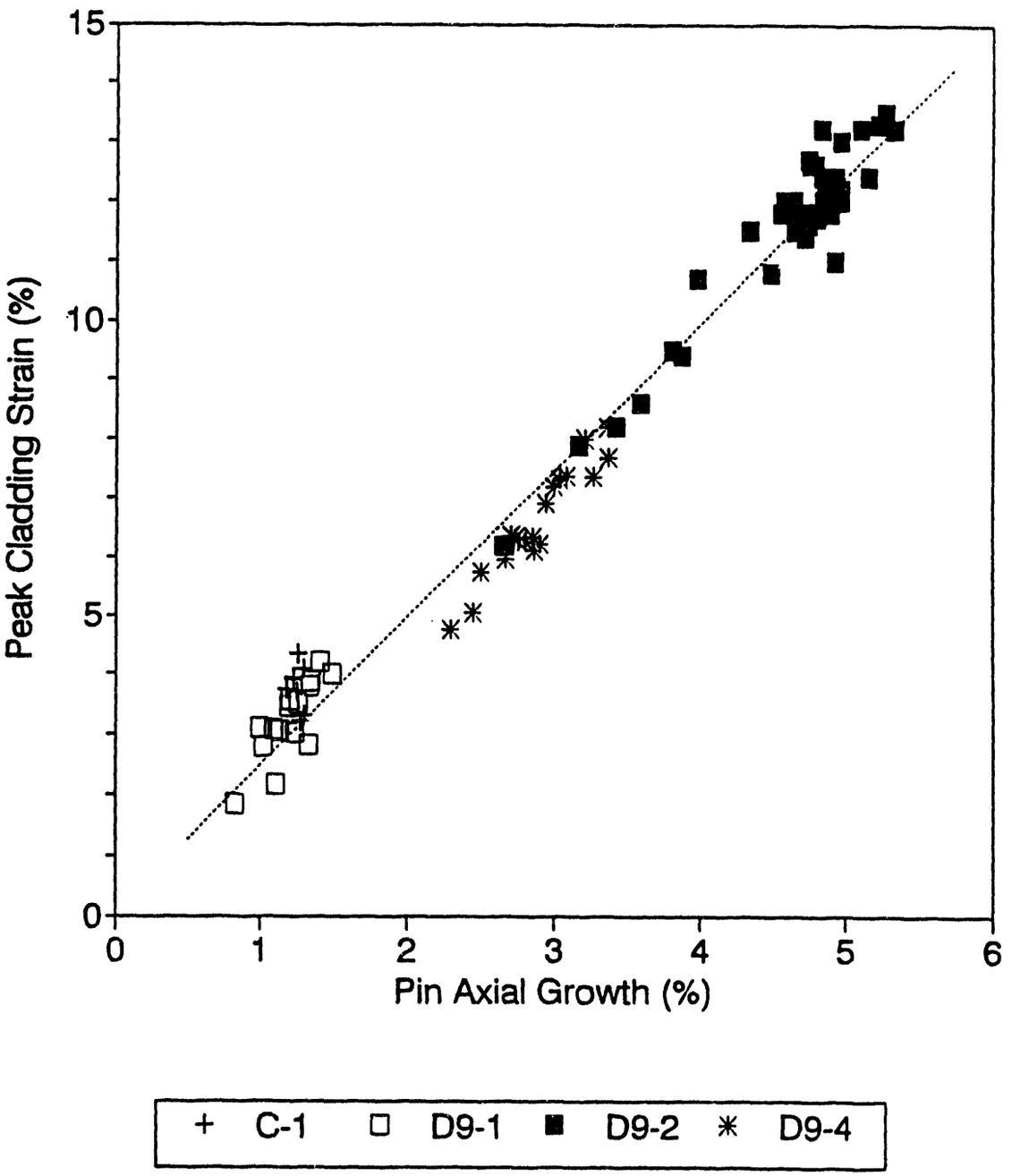

Figure 10. Fuel Column Growth Versus Pin Axial Growth.

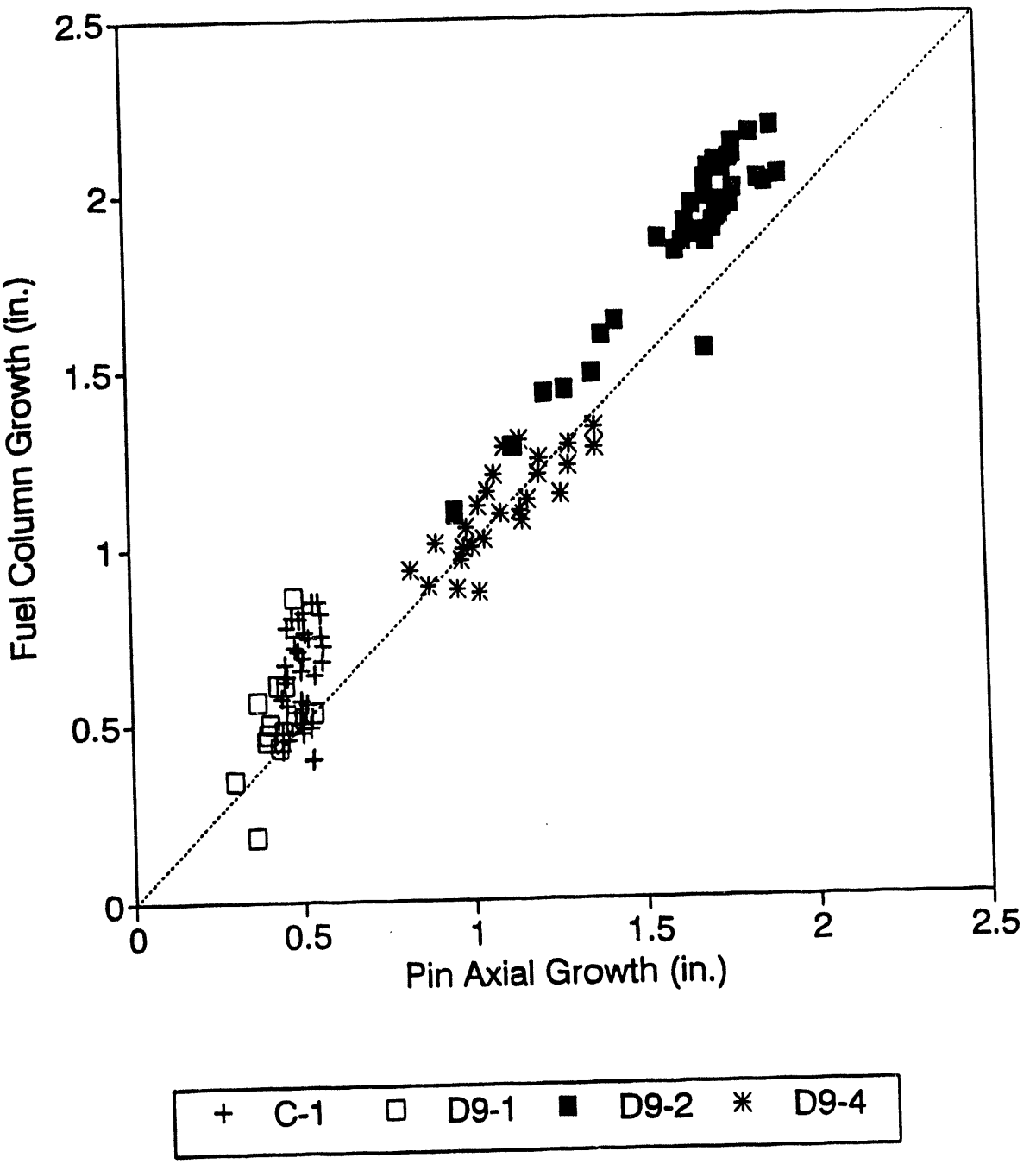

Figure 11. Fission Gas Release Versus Fuel Burnup.

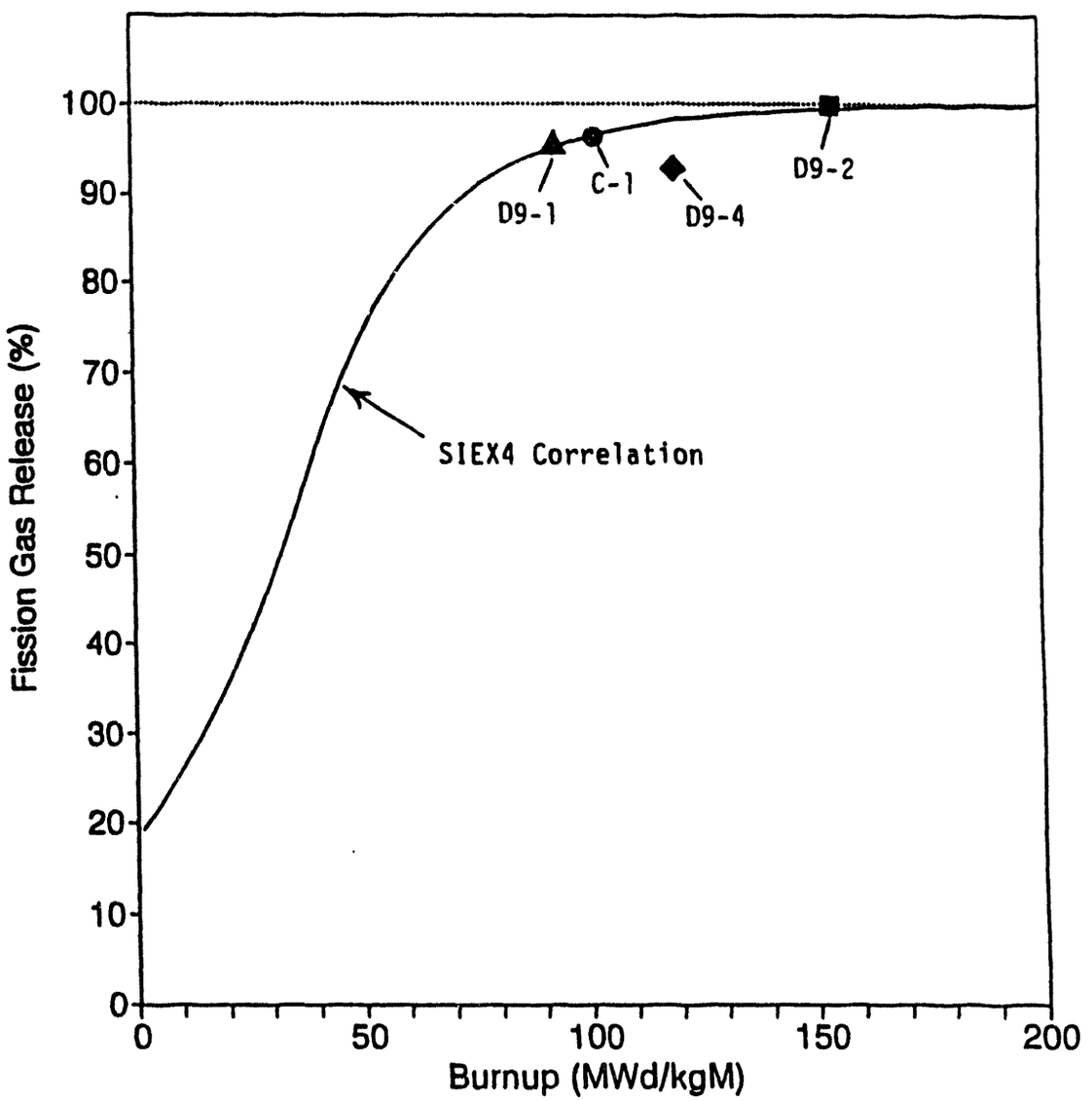

Figure 12. Calculated and Measured Cladding Strain Profiles.

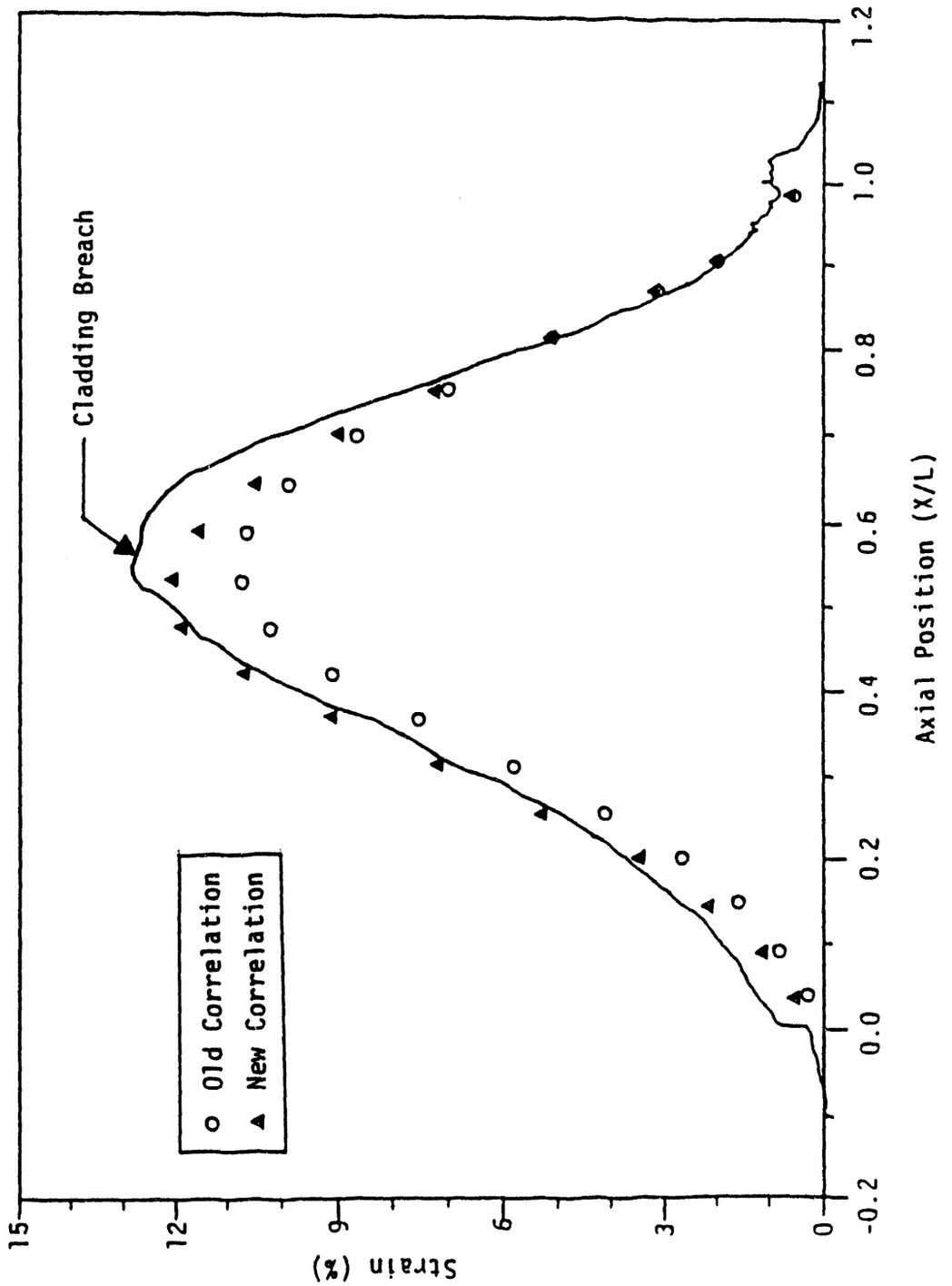

Figure 13. Calculated Versus Measured Peak Cladding Strains.

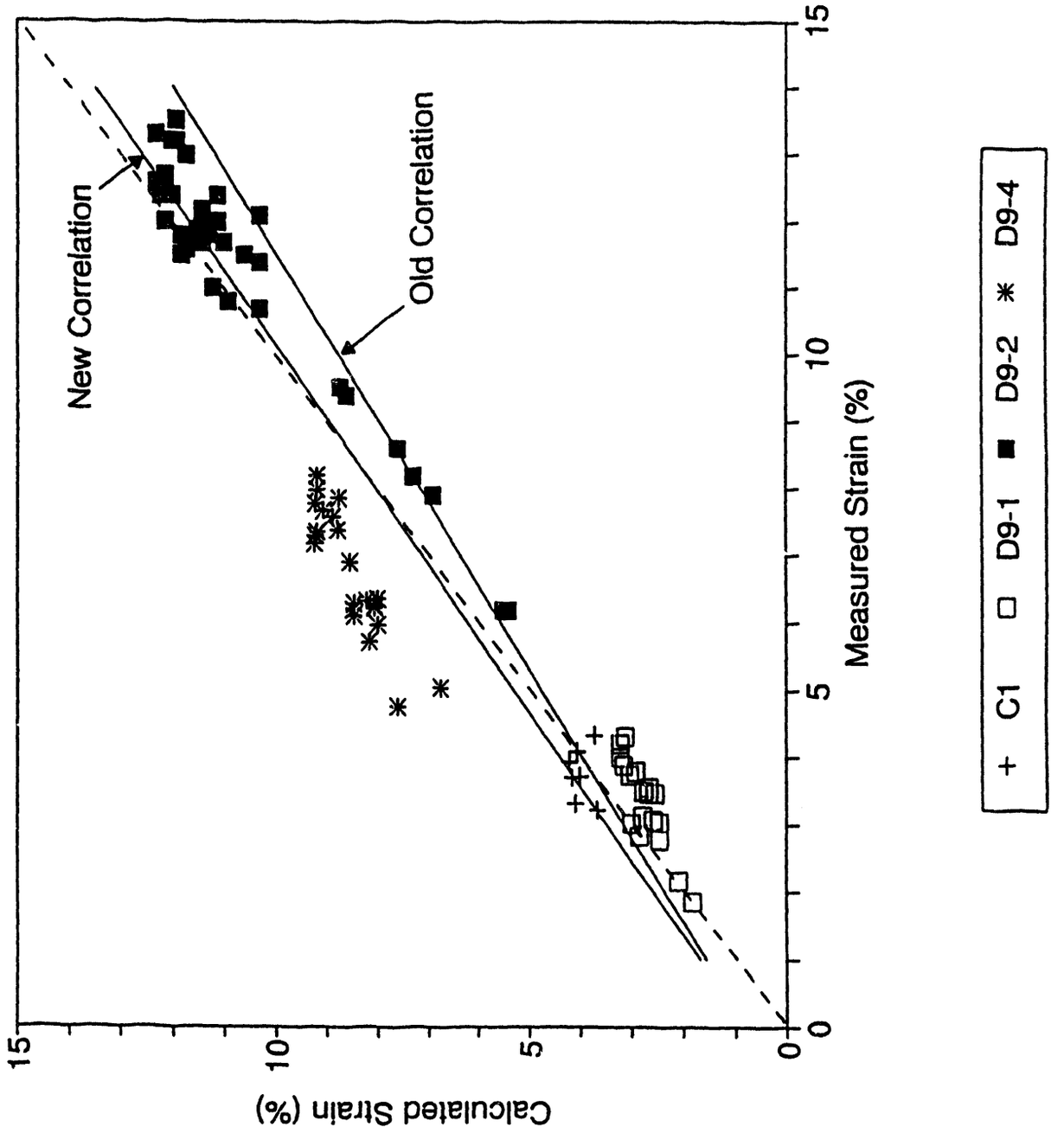

Figure 14. Weibull Failure Analyses Results for 316 SS and D9 Fuel Pins.

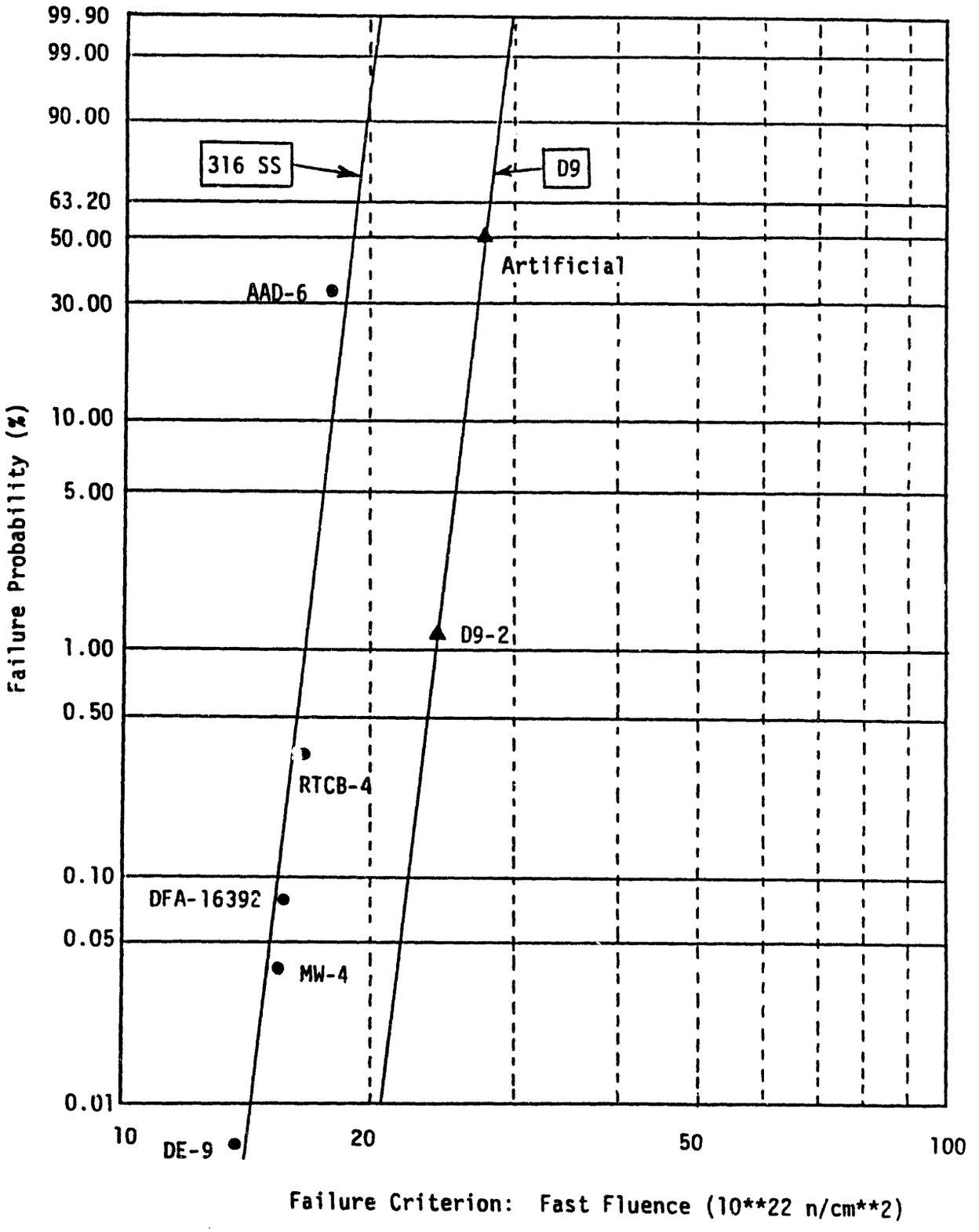

DISTRIBUTION

Number of copies

OFFSITE

1 Oak Ridge National Laboratory
P. O. Box 2008
Oak Ridge, TN 37831-6376

OSTI

ONSITE

2 U.S. Department of Energy
Richland Field Office

O. A. Farabee	N1-39
R. A. Almquist	N1-39

23 Westinghouse Hanford Company

R. B. Baker	L5-01
F. E. Bard	L5-01
K. R. Birney	H0-32
A. E. Bridges	L5-01
S. A. Chastain	L5-01
J. W. Daughtry	N2-32
E. W. Gerber	L5-62
B. C. Gneiting	L5-01
N. J. Graves	L5-01
S. L. Hecht	L5-01
R. A. Karnesky	H0-39
J. A. Lancaster	L5-01
R. D. Leggett	H0-32
B. J. Makenas	L5-02
J. C. Midgett	N2-51
R. P. Omberg	H0-40
A. L. Pitner (2)	L5-01
A. E. Waltar	H0-32
J. D. Watrous	L5-08
Document Processing and Distribution (2)	L8-15
Information Release Administration	L8-07

DATE
FILMED
8/24/94
END